A FODO-BASED NUMI BEAMLINE DESIGN

JOHN A. JOHNSTONE
BEAM PHYSICS

Protons extracted from the Main Injector in the MI60 straight are transported 374 m to the NuMI target. This 120 GeV/c transfer line design is comprised of 4 major sections: an optical matching section between the Injector and transport line; a section of periodic FODO cells; a special straight section insertion across the 67 m drift of the carrier pipe, and; final focusing onto the target. The (predominantly) vertical bending is provided by EPB and B2 dipoles, while 21 quadrupoles of the 3Q60/120 design define the optics.

Three Lambertsons and a C-magnet at Q608 in the MI extract the beam upwards at an angle of 32.6 mr. By powering the 2 Lambertsons plus the C-magnet downstream of Q608 at ~20% above their nominal 120 GeV/c fields sufficient separation is created between the extracted and MI circulating beams to insert a rolled 3Q120 magnet into the slot between the C-magnet and MI quad Q609.

Six rolled EPB's, each bending by 11.4 mr, level the beam off 0.95 m above the MI, but below the Recycler Ring, and steer it onto its final horizontal trajectory. Another seventy meters downstream 6 vertically-bending B2's pitch the beam downwards through the carrier pipe at an angle of 156 mr. A final set of 4 B2's remove 98 mr of this vertical pitch; aligning the beam onto the target 34.3 m further downstream and towards the Soudan detector.

DIPOLES					
String	Type	#	Length (m)	B (T)	Roll
V1	EPB	1 2 2 1	3.048	1.4986	1.61º 33.00º 36.51º 33.00º
V2	B2	6	6.0706	1.7148	90º
V3	B2	4	6.0706	1.6103	90º

Table 1. Magnet parameters of the 3 major bend centers.

Optics

Lattice functions for the transfer line are illustrated in Figure 1. The corresponding beam envelopes and magnet apertures are shown in Figure 2.

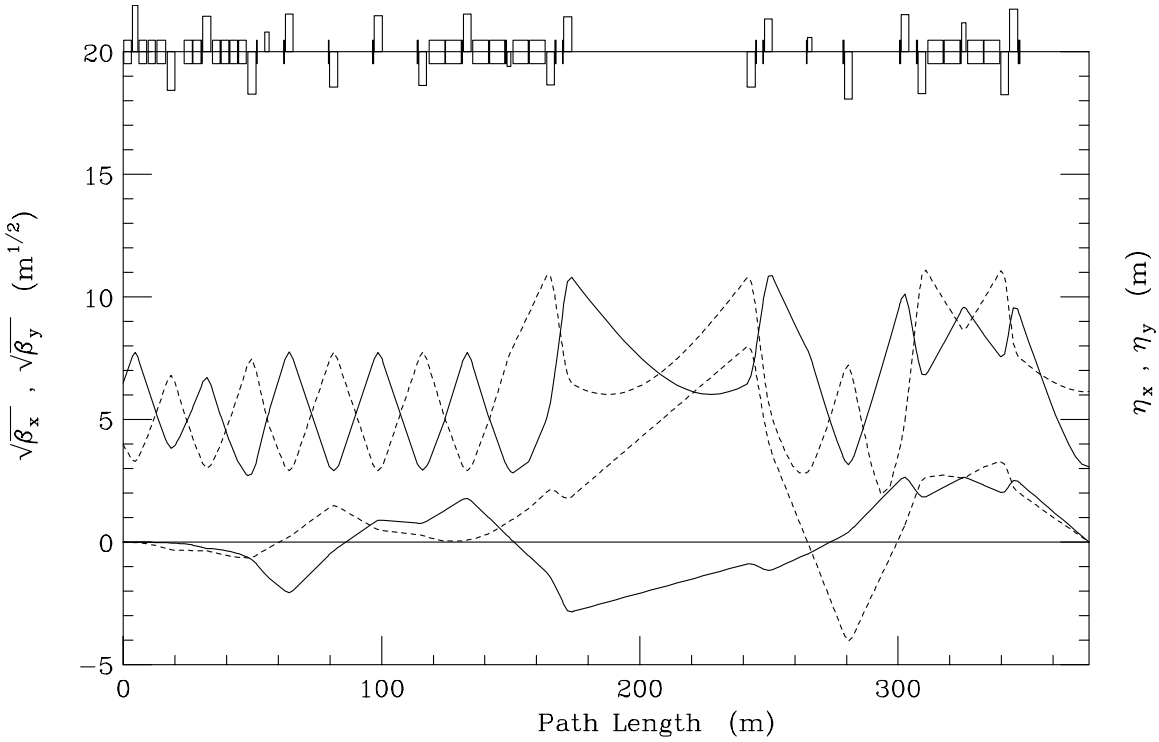

Figure 1. Horizontal (solid) & vertical (dashed) lattice functions of the NuMI transfer line.

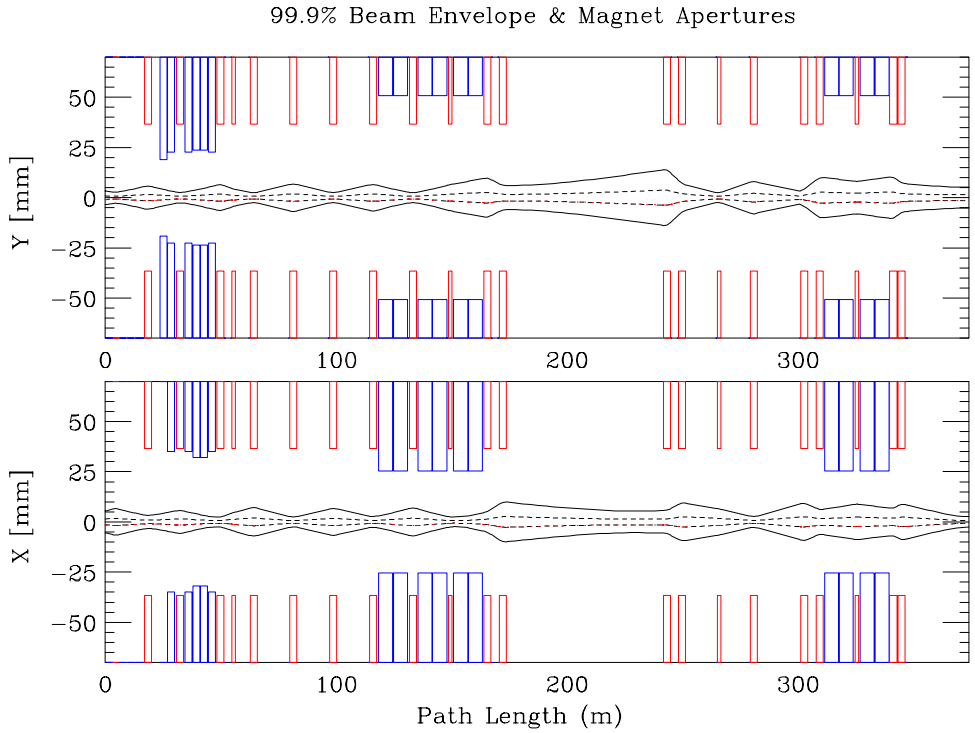

Figure 2. Magnet apertures & beam envelopes [1σ (dashed); 99.9% (solid)] corresponding to a 40π emittance (95%, normalized) beam with $\delta p_{95}/p$ = 7.E-4. (MI components are not shown).

The first 4 quadrupoles in the transfer line are powered individually and optically match the appropriate β's & α's of the MI to those of the transfer line. Through this section β is kept reasonably small in both planes to avoid problems with the tight EPB apertures. The matching section is followed by 86 m of FODO cells characterized by quads Q105 $\rightarrow$ Q109. The half-cell length and phase advance are such that this essentially replicates the MI lattice. Quads Q110, Q111, & Q112 at the upstream end of the long carrier pipe, and Q113, Q114, & Q115 at the downstream end, create straight section optics very similar to those of the Tevatron. Peak β's in the doublets are equal in both planes, with $\beta(\max) \approx 121$ m.

QUADRUPOLES		
Quad #	Length (m)	Gradient (T/m)
Q101	3.048	13.2876
Q102	3.048	12.3403
Q103	3.048	14.6796
Q104	1.524	6.9234
Q105 / 106 / 107 / 108 / 109	3.048	12.3445
Q110 / 115	1.524	5.0768
Q111 / 114	3.048	11.5134
Q112 / 113	3.048	12.1383
Q116	3.048	16.2339
Q117	3.048	12.9807
Q118	3.048	14.5280
Q119	1.524	9.9047
Q120	3.048	14.8634
Q121	3.048	14.8351

Table 2. Quadrupole circuits and parameters.

The last 6 quadrupoles in the line perform the final focus to obtain the desired beam size at the target and also to eliminate dispersion — $\eta_X = \eta_Y = 0$ on the target. With only 1 horizontal bend center in the line plus the additional vertical constraints imposed by the existing tunnel, though, it is not possible to also tune the dispersion slopes to zero. With $\beta_X(\max) \approx 100$ m, and $\beta_Y(\max) \approx 121$ m, aperture restrictions are not an issue through this region. The final focus segment is optically flexible and can comfortably accommodate ±30% β variations in each plane independently.

For the optics solution illustrated in Figure 1, at the target $\beta_X = 9.40$ m, $\beta_Y = 37.60$ m, $\alpha_X = \alpha_Y = 0$, which, for a 40π (95%, normalized) beam gives a spot size of $\sigma_X = 0.70$ mm, and $\sigma_Y = 1.40$ mm. Since the MI emittance at 120 GeV/c is believed currently to be ~25π, and it is not known how this might evolve in the future, it is important that the final focus be sufficiently robust to

produce the desired spot size over a wide range of possible extracted MI emittances. Figure 3 shows the appropriate tuning curves for quads Q118 → Q121 as a function of emittance. Across this spectrum of solutions β_y(max) at Q118 never exceeds ≈ 144 m, corresponding to less than a 10% increase in beam size over the nominal 40π case.

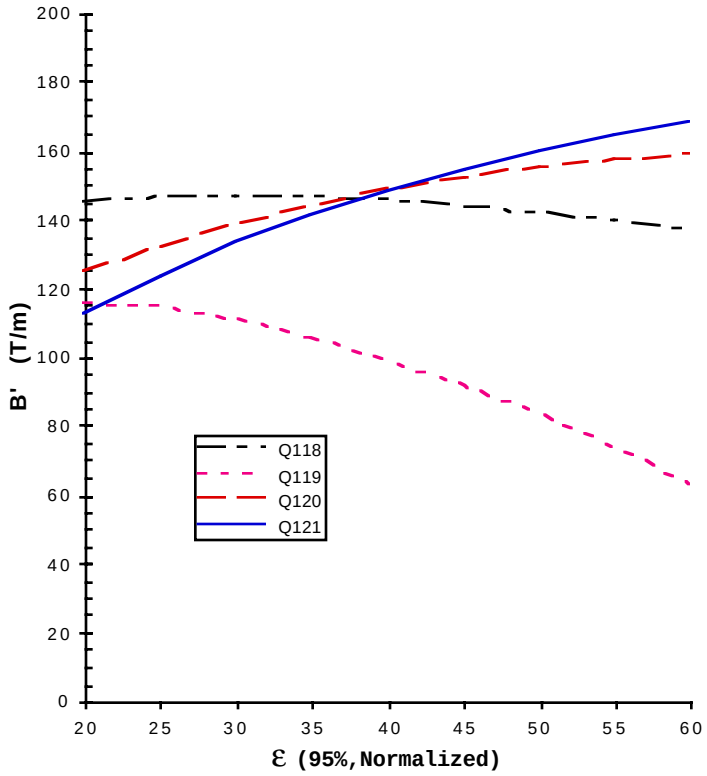

Figure 3. The Q118 → Q121 gradients that produce σ_x = 0.70 mm, σ_y = 1.40 at the target as beam emittance varies.

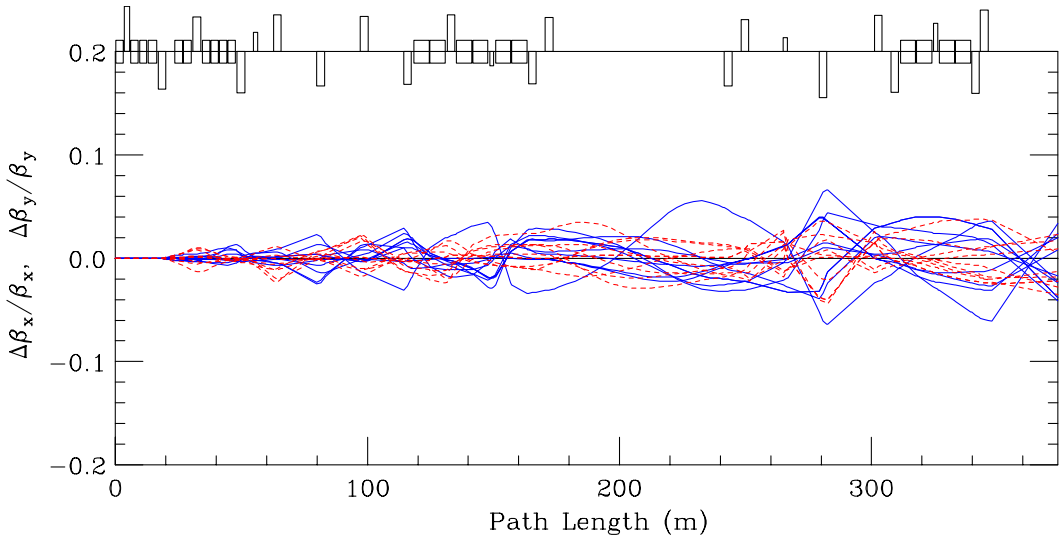

Figure 4. The effect on β due to random gradient errors with σ(ΔB'/B') = 25E-4.

The sensitivity of the optics to different error sources has been studied in simulations. Assigning random gradient errors of σ(ΔB'/B') = 25E-4 to the 21 quadrupoles in the line, Figure 4 shows the relative β-waves that result from 10 random generator seeds. The β-wave accumulates progressively down the line but Δβ/β never exceeds ≈6%, which translates into an ≈3% increase in beam size at most. This is confirmed in Figure 5 where, for the same 10 seeds, the change in σ's are seen to be less than ≈60 μm. At the target the maximum changes in beam size are on the order of 20–30 μm.

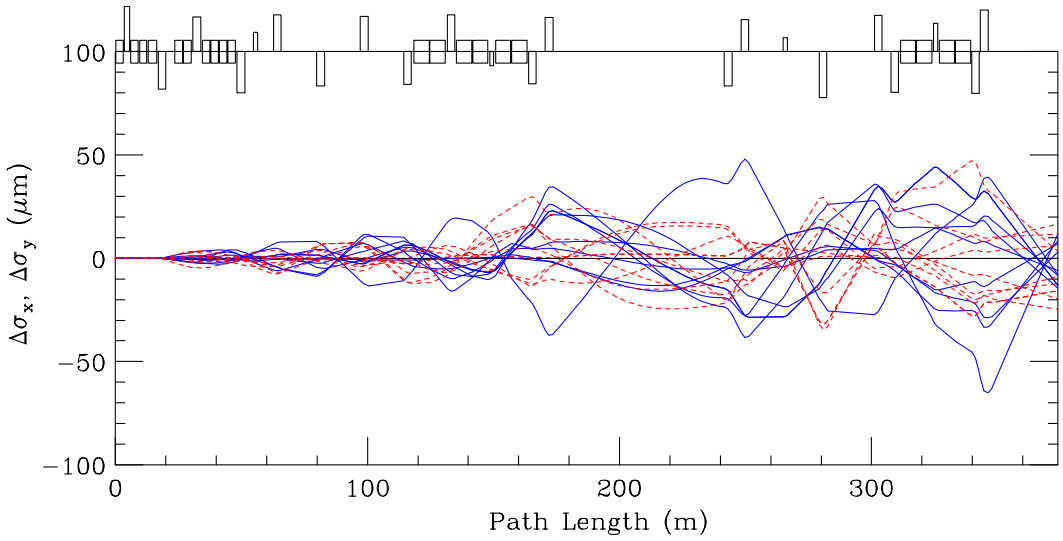

Figure 5. Beam size variation resulting from random gradient errors.

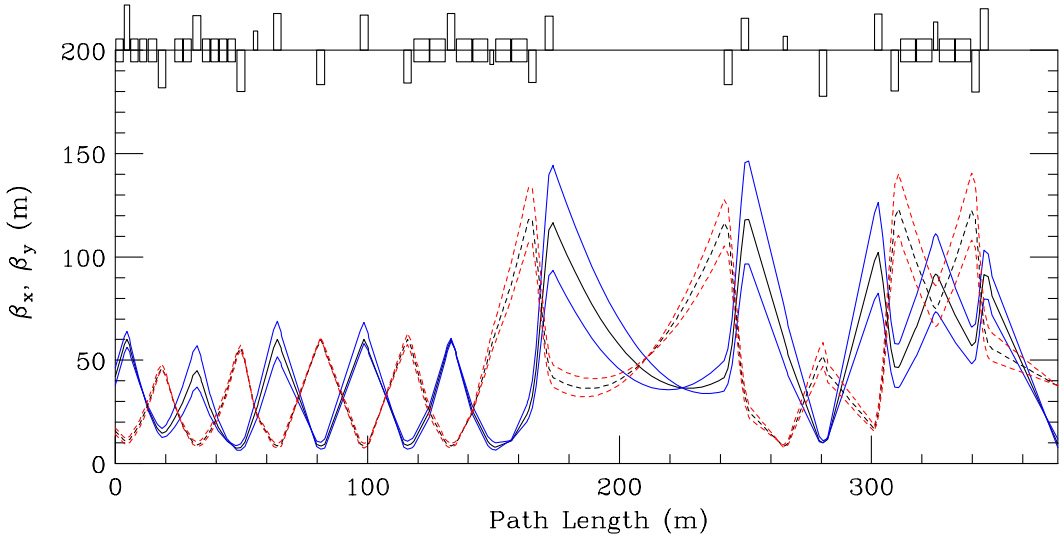

Figure 6. β-waves due to ±10% injection optic errors.

The beamline is not overly sensitive to injection optics errors. Figure 6 shows the β-envelopes that result from ±10% variations in the nominal β_X & β_Y injection values. The MI-end matching section can be re-tuned to eliminate these mismatchs, but it can be seen that this isn't strictly necessary — the maximum β's are sufficiently well-behaved that no aperture problems arise, and the small residual mismatch at the target can easily be corrected by the 4 final-focus quadrupoles.

Trajectory Correction

Every focusing element in the line has a BPM associated with it, and both horizontal & vertical BPM's are assigned to the first quad, Q101. Every quadrupole, with the exceptions of Q101 & Q104, also has a MI-style dipole corrector nearby. Space limitations at Q101 preclude installing a corrector, while for Q104 there are already correctors in both planes closeby at Q103 & Q105. Orbit correction is an issue which, of course, must be addressed by any beamline, but for the ultra-clean transport requirements of NuMI it is critical that sensitive position control is available throughout the line.

Correction of central trajectory errors has been simulated with random magnet misalignments and dipole field errors assigned to the beamline elements. Suitable error values are $\sigma(\Delta x, \Delta y) = 0.25$ mm, $\sigma(\psi_{roll}) = 0.50$ mr, and $\sigma(\Delta B/B) = 25E\text{-}4$. Figure 7 illustrates deviations of the central trajectory for 10 random error seeds. The uncorrected offsets in the line are $\Delta x(rms) = 1.24$ mm, $\Delta x(max) = 6.94$ mm, and $\Delta y(rms) = 1.47$ mm, $\Delta y(max) = 6.27$ mm.

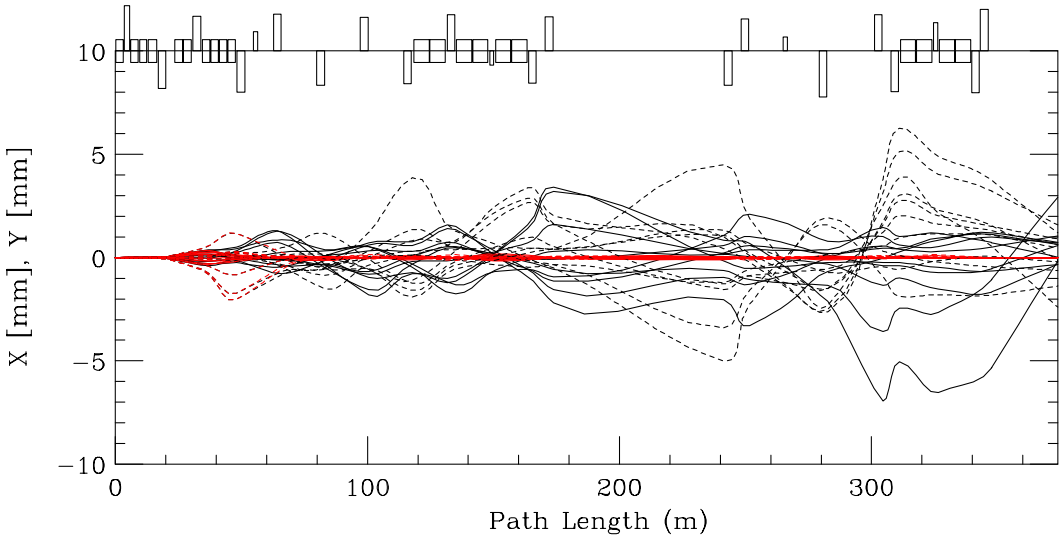

Figure 7. Uncorrected & corrected trajectories resulting from random magnet misalignments and dipole field errors

The corrected orbits are also shown in Figure 7 in red. After correction the trajectory deviations are reduced to $\Delta x(rms) = 0.07$ mm, $\Delta x(max) = 0.33$ mm, $\Delta y(rms) = 0.25$ mm, $\Delta y(max) = 2.02$ mm, and the beam position and angle at the target are tuned to $\Delta x = \Delta y = 0$ mm, $\Delta x' = \Delta y' = 0$ μr. Maximum x & y deviations occur at Q102 & Q103, respectively. This is simply a reflection of the fact that position control at those locations requires tuning the MI kickers, Lambertsons & C-magnet — refinements not included in the present simulations.

The corrector strengths required are $\theta_X(rms) = 16.14$ μr, $\theta_X(max) = 52.90$ μr, and $\theta_y(rms) = 21.10$ μr, $\theta_y(max) = 68.47$ μr. Horizontal values are well below the 150 μr available at 120 GeV/c. The maximum vertical kick, however, is uncomfortably close to the maximum 75 μr attainable from a MI-style vertical corrector. Possible solutions are either to re-align magnets, or install rolled horizontal correctors in some locations.

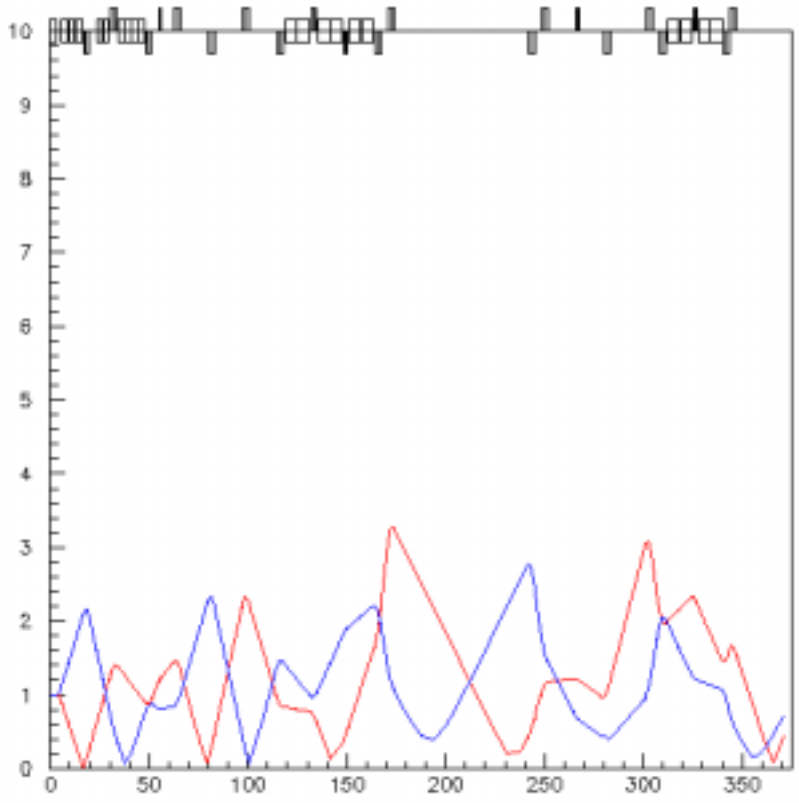

Figure 8. Envelopes of possible trajectories arising from injection errors of (Δx, Δy) = ±1 mm and central momentum error $\delta p_{95}/p_o = 1.E\text{-}4$.

While dipole correctors are essential to compensate systematic, time-independent trajectory errors, they are of no use in addressing pulse-to-pulse MI extraction variations. Tracking studies[1] with realistic injection position errors of ±1 mm in each plane, plus MI central momentum errors of $\delta p_{95}/p$ = 1.E-4 yield the envelopes of possible trajectories depicted in Figure 8. The maximum excursions of ~3 mm horizontally & vertically do not pose any aperture difficulties and, in fact, it can be seen that the offset error on the target is somewhat less than the initial injection error.

[1] T. Kobalarcik, "Comparison of Solutions for the NuMI Beamline", Internal Report, 2002.